



Large Scale CO Survey of the Northern Galaxy

-Preliminary results at L=(13.2,16.3) and B=(-1.2,0.2)



Zhibo Jiang^{1,2}, Junyu Li^{1,2,3,*}

1. Purple Mountain Observatory, Nanjing, 210008, China
2. Key Laboratory of Radio Astronomy, Chinese Academy of Sciences, Nanjing 210008, China
3. Graduate School, Chinese Academic of Sciences, Beijing 100049, China

Abstract: We present the ^{12}CO , ^{13}CO and C^{18}O line survey towards a region of $L=(13.2,16.3)$ and $B=(-1.2, 0.2)$, as a part the ambitious project, the Milky Way Image Scroll Painting. The CO line emissions show a number of velocity components, each component shows different structure and morphology than the others. A common feature that shows up in every component is the filamentary structure. Meanwhile a number of bubbles are found in some components, which are especially clear at 40 km s^{-1} and 60 km s^{-1} . The velocity gradient of the 20 km s^{-1} component is surprisingly large, which can be interpreted neither by simply assuming the global rotation of the spiral arms nor by assuming the local motion along the spiral arm.

1. Introduction

With the accomplishment and commissioning of the Superconducting Spectroscopic Array Receiver (SSAR, Shan et al. 2012), the efficiency of the Delingha millimeter telescope has been greatly increased. Presently it can observe the CO and its isotopic molecular lines (^{12}CO , ^{13}CO and C^{18}O , $J=1-0$) simultaneously with 9 beams. With the On-the-Fly (OTF) scanning mode, the telescope provides a mapping speed up to $1/8$ square degree per hour at high elevations, and half of that at low elevations, rendering rms noises of $\Delta T_{\text{R}}^* \sim 0.5 \text{ K}$ at upper side-band and $\sim 0.3 \text{ K}$ at lower side-band. Under such circumstance the Purple Mountain Observatory initiated a large-scale CO survey toward the northern Galactic plane, which is called the Milky Way Image Scroll Painting (MWISP). The project aims to map the Galactic plane with $-10 \leq L \leq 260$, $|b| \leq 5$, in about 8 years.

As a part of MWISP, we present here the preliminary result of the observations toward a field of $13.2 < L < 16.3$ and $-1.2 < B < 0.2$. Our initial motivation was to investigate the giant molecular cloud being associated with the M17 star forming region. However, the result presented here has been extended far more than that region, reaching an area of ~ 4.5 square degrees.

2. Observation and data reduction

The observations were carried out between November and December 2011, using the Delingha 13.7m millimeter telescope with the SSAR. The telescope can provide ^{12}CO , ^{13}CO and C^{18}O $J=1-0$ line observations simultaneously; ^{12}CO line is put into the upper side-band while ^{13}CO and C^{18}O lines are put into the lower side-band. Following the rule of MWISP, whole observation field is split into "cells"; each cell is 30 by 30 square arcmin. The observations used OTF mode. The scanning speed was set to $0.2''$ per second. Each cell has been scanned for twice, one along the galactic longitude and one along the latitude. The typical system temperatures were about 280 K and 150 K for upper- and lower- sideband, respectively. This schedule results in a typical RMS noise temperature (corrected for main beam efficiency and atmospheric effects) of 0.5 K and 0.25 K for upper- and lower- sideband, respectively (Fig. 1).

The raw data were checked for bad beams and bad channels at first, and then reduced by pipeline written in GILDAS/CLASS package, cell by cell. The pipeline used first order baseline fitting. The data were then re-gridded into 26 arcsec (nearly half size of the main beam) per pixel. After all cells were reduced, the whole set of the data were mosaicked into a FITS file for further analysis.

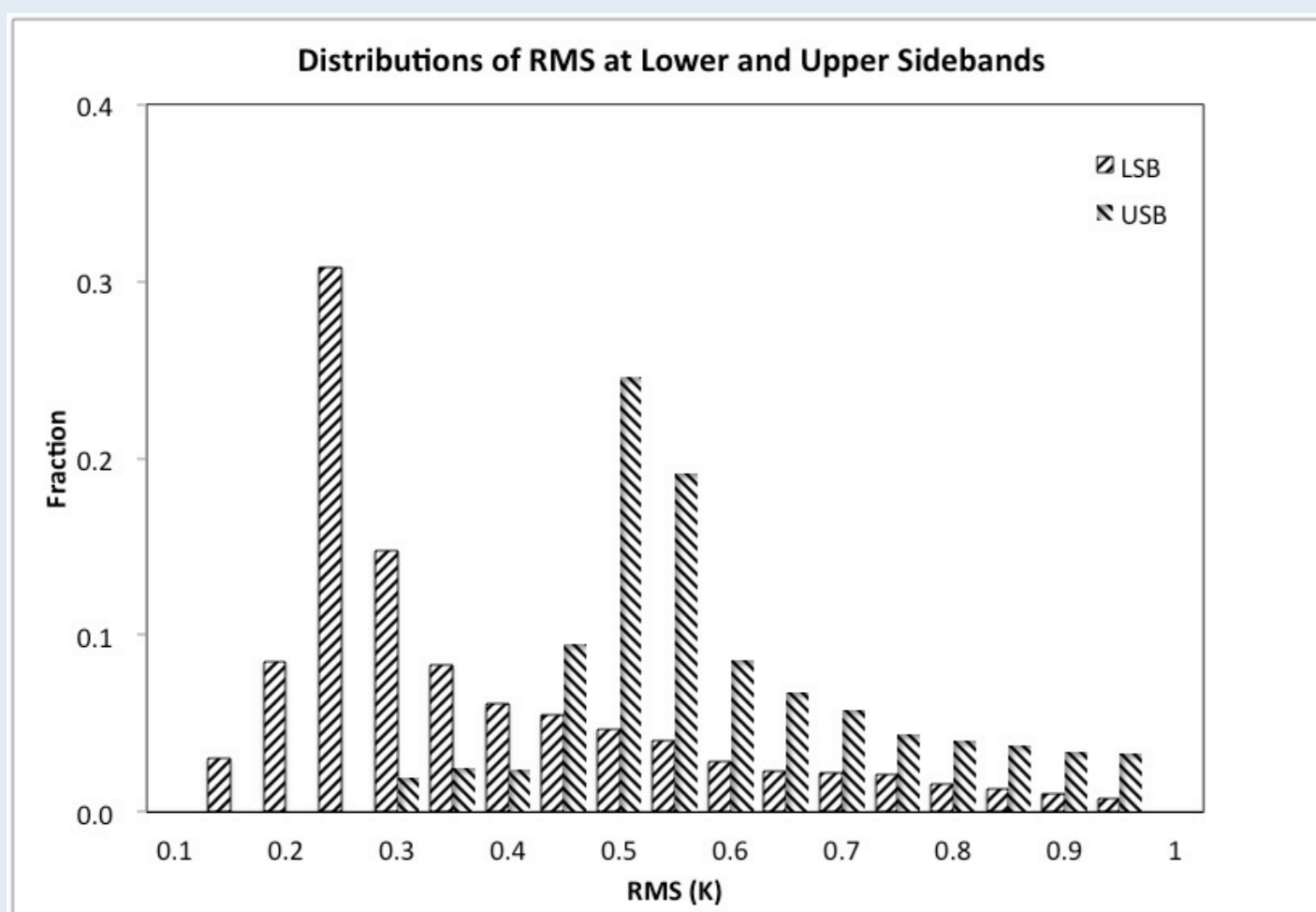


Fig. 1 (up) The RMS distribution of the lower- and upper- sidebands. The statistics is made from all pixels observed ($26'' \times 26''$, 0.167 km s^{-1} , for lower sideband, 0.159 km s^{-1} for upper sideband.)

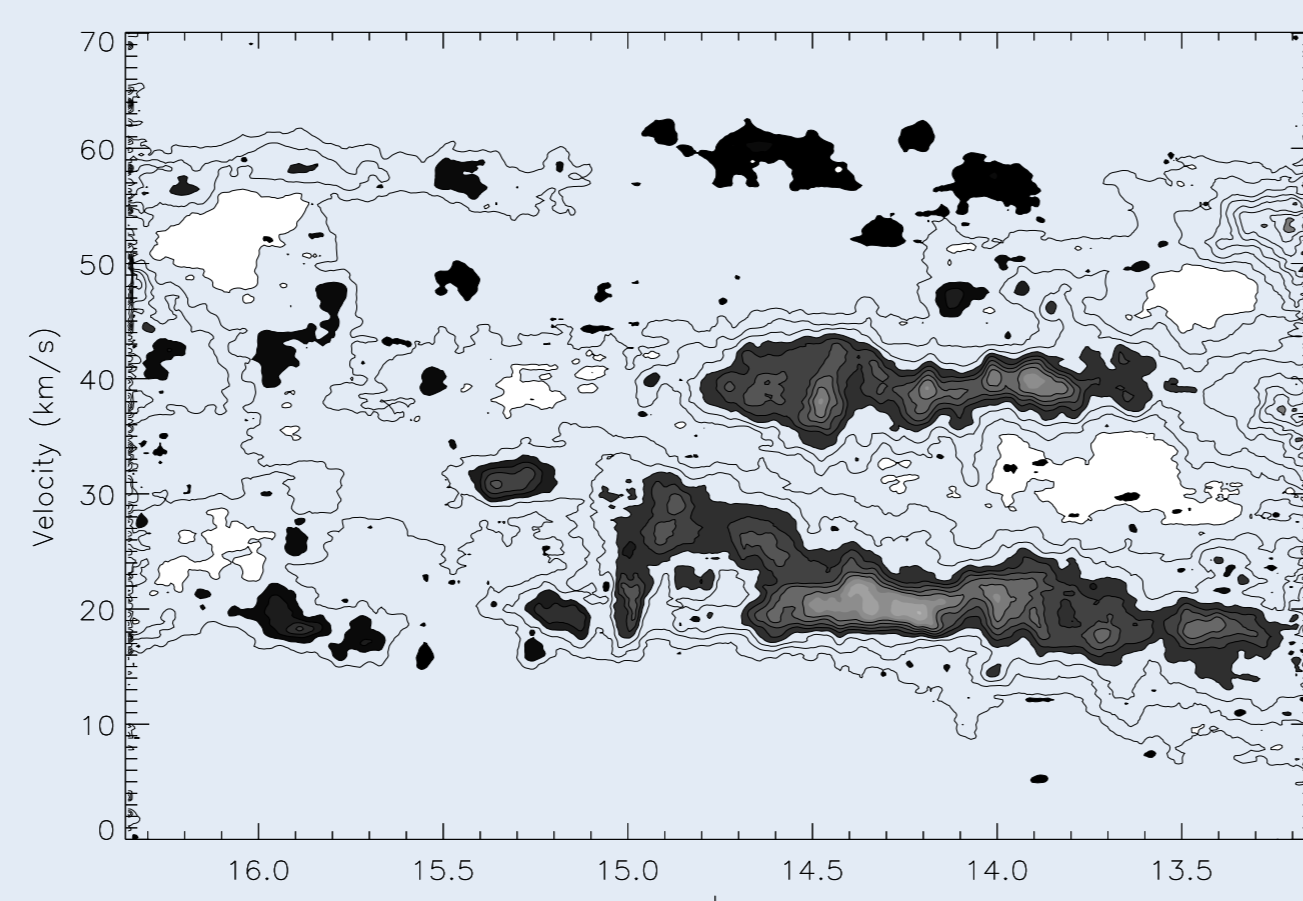
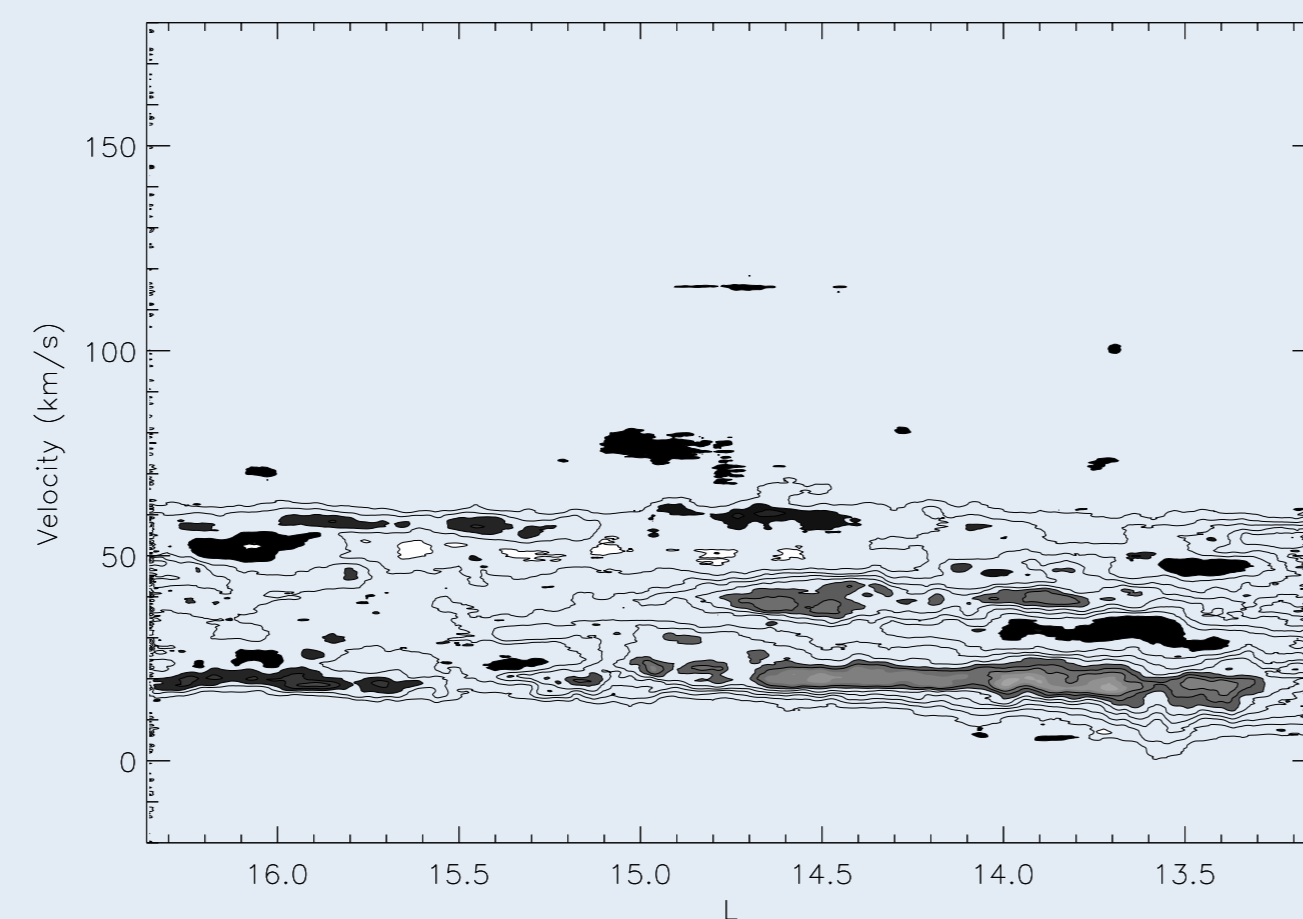


Fig. 2 ((right)) The position-velocity diagrams of ^{12}CO (upper) and ^{13}CO (lower) along the galactic longitude. The data have been averaged over a latitude $b = -1.2 - 0.2$.

3. Results and discussions

Fig. 2 shows the position-velocity (P-V) diagrams of ^{12}CO and ^{13}CO . We averaged lines along the galactic latitude between $b=-1.2$ and $b=0.2$, for higher signal-to-noise ratios. Fig. 2 clearly demonstrates three main streams along the longitude direction; they are at the velocity of $\sim 20 \text{ km s}^{-1}$, $\sim 40 \text{ km s}^{-1}$ and 60 km s^{-1} . Calculating the kinematical distances of each component suggests they could be located in the Sagittarius arm, Scutum-Centaurus arm and Norma arm, respectively. Apart from those three main streams, other components at $\sim 75 \text{ km s}^{-1}$ and $\sim 120 \text{ km s}^{-1}$ are detected. They are presumably other farther arms of the Galaxy.

In the lower-panel of Fig. 2, we present the P-V map of ^{13}CO , between the velocity range $[0,70]$ (km s^{-1}). The 60 and 40 km s^{-1} components generally show a slow rise towards greater longitude. This could be fairly accounted by global rotation of the Galaxy. On the other hand, the 20 km s^{-1} component shows a larger velocity gradient towards increasing longitude. This is particularly clear between $L \sim [13.2, 15.5]$. A weighted linear fit of the $L-v$ correlation, assuming the antenna temperatures (TR^*) as the fitting weights, suggests a very large velocity gradient, i.e., $v = -41.9 + 4.4L$. Such a large gradient cannot be interpreted by merely assuming the circular motion at a velocity of $\sim 200 \text{ km s}^{-1}$. Further, any assumption the local gas flow along the spiral arm can account for such a large value neither. The only possible reason left seems to lie on the assumption of large-scale rotation of the molecular complex. However, it is quite a mystery for us how such a large-rotation rotation could exist.

*The people who are involved in the whole project:

J. Yang, Y. Xu, H.C. Wang, R.Q. Mao, M. Wang, Y. Su, M. Fang, Y. Wang, Y. Liu, X. Zhou, S.B. Zhang, X.J. Shao, X. Liu, Y. Sun, Y. Gong

This project is supported by the Natural Science Foundation of China through 11233007

In Fig. 3 we present the maps of the CO emissions. The first three panels are color-coded images different velocity components. The color images are composed from the integrated intensities of the ^{12}CO (blue), ^{13}CO (green) and C^{18}O (red) emissions, integrated over the velocity ranges shown on tops of the panels. The other three panels are ^{12}CO emissions over the respective v -ranges. These images clearly show different component has different structure and morphology.

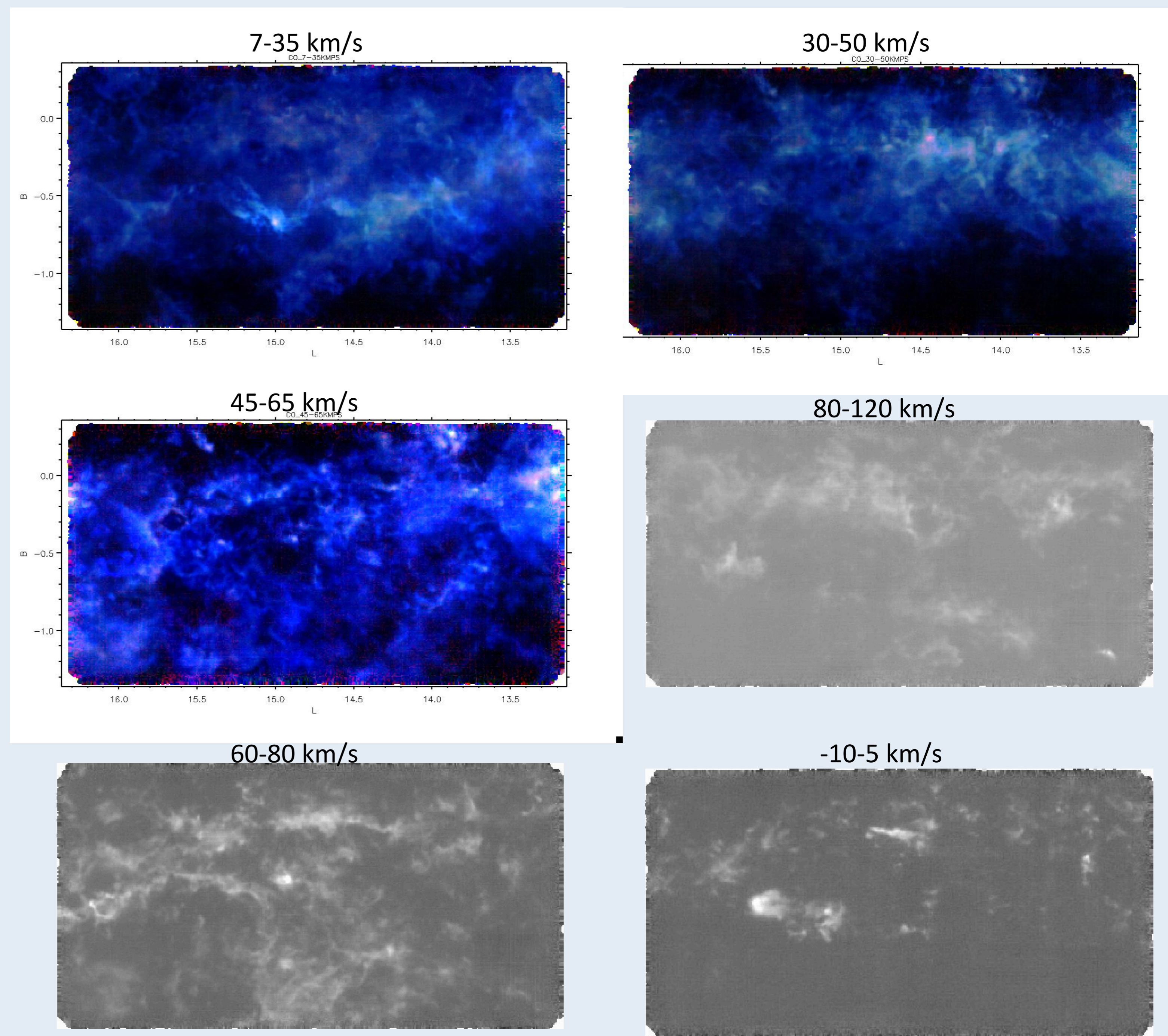


Fig. 3. Integrated intensity images. The first three color images are composed from the ^{12}CO (blue), ^{13}CO (green) and C^{18}O lines, while the other three are only ^{12}CO emissions because in the given velocity range C^{18}O emissions are not detected or have poor s/n ratios. The velocity ranges for the integration are shown on tops of the panels.

L	B	Vc (km/s)	size (arcmin)	Moph.	Arm
13.26	-0.35	41.7	6.5	cir	2
13.29	-0.32	41.7	9.4	ellip	2
13.37	-0.49	34.5	3.9	cir	2
13.5	-0.08	40.4	9.9	irr	2
13.67	0.04	40.4	8.5	irr	2
13.7	-0.06	41.2	5.7	cir	2
13.82	-0.3	57.6	7.6	ellip	3
14.06	-0.56	58.4	5.5	cir	3
14.27	-0.14	61.3	5.4	cir	3
14.32	-0.13	56.0	5.4	cir	3
14.35	-0.05	54.6	5.5	cir	3
14.38	-0.41	74.8	8.7	cir	1
14.44	-0.5	59.1	4.5	cir	3
14.56	-0.35	59.8	4.0	cir	3
14.56	-0.13	61.3	8.0	ellip	3
14.6	-0.29	41.2	6.8	ellip	2
14.61	-0.11	37.5	3.0	cir	2
14.62	-1.03	36.7	6.5	irr	2
14.69	-1.12	35.2	6.5	irr	2
14.72	-0.99	35.2	6.5	cir	2
14.8	-0.62	46.4	4.3	irr	2
14.81	-0.04	55.3	7.0	irr	3
14.92	-0.23	41.2	6.8	irr	3
14.93	-0.31	44.1	5.4	irr	3
14.96	-0.43	44.2	12.0	ellip	3
15.06	0.35	29.2	18.0	part	1
15.38	-0.36	20.3	16.2	irr	1
15.46	-1.02	15.1	7.5	irr	1
15.58	-0.83	15.8	6.6	irr	1
15.67	0.09	33.0	3.3	cir	1
15.84	0.11	51.2	9.1	ellip	2
15.89	-0.39	42.4	7.4	cir	2
15.97	-0.02	12.8	6.2	cir	1
16.11	-0.18	101.6	4.4	cir	4

Table 1. Molecular bubbles identified by visual inspections. Arm codes: 1- 20km/s arm; 2- 40 km/s; 3- 60 km/s; 4- other.

An interesting feature of the integrated intensity images is the widely existed bubble-like structures. By visual inspections, we could identify a number of bubbles, which are listed in Table 1. Since these bubbles are identified visually, it is hard to say that they are complete. However, the existence of such a large number of bubbles in such a small region would suggest the it is bubblier over the whole Galaxy, as suggested by Simpson et al. 2012.

Conclusions:

1. We have carried out a CO line survey toward a region between $L \sim 13.2 - 16.3$ and $b \sim -1.2 - 0.2$, with ^{12}CO , ^{13}CO and C^{18}O $J=1-0$ lines.
2. These lines show a number components. The main components are at the velocities $\sim 20, 40$ and 60 km s^{-1} , corresponding to Sagittarius arm, Scutum-Centaurus arm and Norma arm. Other components are also detected in ^{12}CO but not in C^{18}O line.
3. The components show different structures and morphologies.
4. The P-V diagram shows an unusual velocity gradient, suggestive of large-scale rotation of the molecular complex.
5. We detected a number of molecular bubbles in the region.

1. Deharveng, L. et al. 2010, A&A, 523, A6
2. Shan, W.L. et al. 2012. IEEE Transactions on Terahertz Science and Technology, Vol2, issue 6, pp593-604
3. Simpson, R.J. et al. 2012, MNRAS, 424, 2442
4. Xu, Y. et al. 2011, ApJ, 733, 25
5. Zuo, Y.X. et al. 2011. Chinese Astro. Astrophys. Vol 35, pp439-446